Article

Investigation of Hydrodynamic Parameters in an Airlift Photobioreactor on CO_2 Biofixation by *Spirulina* sp.

Zahra Zarei [1], Peyman Malekshahi [1], Antoine P. Trzcinski [2] and **Mohammad Hossein Morowvat [3,4,*]**

1   Department of Chemical Engineering, University of Sistan & Baluchestan, Zahedan P.O. Box 98167-45845, Iran; zahrazarei02@gmail.com (Z.Z.); malekshahipayman@gmail.com (P.M.)
2   School of Civil Engineering and Surveying, University of Southern Queensland, West Street, Toowoomba QLD, 4350, Australia; antoine.trzcinski@usq.edu.au
3   Pharmaceutical Sciences Research Center, Shiraz University of Medical Sciences, Shiraz P.O. Box 71468-64685, Iran
4   Department of Pharmaceutical Biotechnology, School of Pharmacy, Shiraz University of Medical Sciences, Shiraz P.O. Box 71468-64685, Iran
*   Correspondence: mhmorowvat@sums.ac.ir; Tel./Fax: +98-71-324-267-29

Abstract: The rise of CO_2 concentration on Earth is a major environmental problem that causes global warming. To solve this issue, carbon capture and sequestration technologies are becoming more and more popular. Among them, cyanobacteria can efficiently sequestrate CO_2, which is an eco-friendly and cost-effective way of reducing carbon dioxide, and algal biomass can be harvested as valuable products. In this study, the hydrodynamic parameters of an airlift photobioreactor such as gas holdup, mean bubble diameter and liquid circulation velocity were measured to investigate CO_2 biofixation by *Spirulina* sp. The total gas holdup was found to increase linearly with the increase in the gas velocity from 0.185 to 1.936 cm/s. The mean bubble velocities in distilled water only and in the cyanobacterial culture on the first and sixth days of cultivation were 109.97, 87.98, and 65.89 cm/s, respectively. It was found that shear stress at gas velocities greater than 0.857 cm/s led to cyanobacterial death. After 7 days of batch culture, the maximum dry cell weight reached 1.62 g/L at the gas velocity of 0.524 cm/s, whereas the highest carbon dioxide removal efficiency by *Spirulina* sp. was 55.48% at a gas velocity of 0.185 cm/s, demonstrating that hydrodynamic parameters applied in this study were suitable to grow *Spirulina* sp. in the airlift photobioreactor and remove CO_2.

Keywords: airlift photobioreactor; carbon sequestration; CO_2 biofixation; gas holdup; liquid circulation velocity; *Spirulina* sp.

1. Introduction

Global warming caused by human activities is one of the significant environmental problems that has received much attention in the last two decades. One of the reasons for the increase in temperature and global warming is the presence of greenhouse gases, especially the high concentration of carbon dioxide in the Earth's atmosphere [1]. This concentration was 260–280 ppm before the industrial revolution, and it has increased significantly since then, reaching 381 ppm in 2005. In the last 100 years, the air temperature has increased between 0.18 and 0.74 °C [2]. A few researchers reported an annual increase of 0.2 °C in the Earth's temperature over the last three decades due to CO_2 emissions, which reached a new record (37%) compared to the late 18th century [3].

Among various methods for reducing CO_2 such as physical absorption, chemical fixation, soil carbon sequestration, biochar and CO_2-enhanced oil recovery, the biological fixation of CO_2 by photosynthetic cyanobacteria have gained attention as an environmentally friendly and economically competitive technology [4–7]. The process requires knowledge of cell biology and factors influencing this process such as temperature, pH, light, cyanobacteria species, cyanobacterial culture density, CO_2 concentration, photobioreactor hydrodynamic parameters (reactor configuration, sparging rate, mixing) [8,9].

However, CO_2 fixation by cyanobacteria on a large scale remains challenging due to the limitation of cyanobacterial growth at high concentrations of CO_2 and the need for more nutrients and light [10,11]. Therefore, selecting suitable cyanobacteria species to thrive at high CO_2 concentrations is considered an essential step in the biological removal of CO_2 [10,12]. *Spirulina* sp. is an ideal candidate due to its resistance to harsh environmental conditions, high CO_2 fixation ability, and growth rate [13,14]. For instance, the removal efficiency of CO_2 fixation by *Spirulina platensis* at 5% CO_2 in the feed gas was found to be 81% in a semi-continuous process [15]. Also, using 6% and 12% CO_2, the maximum CO_2 biofixation by *Spirulina* sp. was 53.3% and 45.6%, respectively [16]. Other researchers observed that the maximum CO_2 removal efficiency by *S. platensis* at 4% and 6% CO_2 was 70% and 65%, respectively, in a tubular photobioreactor [17,18]. Soletto et al. [19] reported that the maximum carbon dioxide removal efficiency of *S. platensis* at 80 and 125 mol photons $m^{-2} s^{-1}$ reached 50% and 69%, respectively, in a bench-scale helical photobioreactor; however, at 166 mol photons $m^{-2} s^{-1}$, the CO_2 biofixation was higher than 90%.

Typical photobioreactors (PBRs) such as vertical column reactors (bubble column and airlift reactors), flat plate, and tubular reactors have been used to achieve high productivity, uniform mixing, high area-to-volume ratio, high light utilization efficiency, and adequate temperature and light control which are desirable characteristics [20,21]. Airlift reactors (ALRs) are ideal for CO_2 biofixation due to good mixing, high mass transfer rate, low shear stress. They also require lower energy input and can be used in a wide range of inlet gas flowrates and higher viscosity fluids [22–24]. Like in bubble columns, agitation is achieved through pumping air which provides low shear stress and high mass transfer [25,26]. ALRs with an internal loop consist of 4 main parts:

(i) the riser (draft tube) is the most important part of the reactor where most of the mixing and mass transfer occurs. The gas distributor is located at the bottom of this section and a directional multiphase flow is created upwards in this area.

(ii) the downcomer works in parallel with the riser and is the external tube. The density in this part is higher than the riser, which causes the fluid to move.

(iii) the sparger (or gas distributor) is located at the bottom of the reactor where the riser and the downcomer are connected.

(iv) the gas separator connecting the two sides of the reactor at the top and the gas separation operation is performed there [24,25]. In airlift reactors, the gas holdup, which depends on reactor height and the gas-liquid separation area in the reactor headspace, is one of the key parameters in determining the liquid circulation velocity, gas residence time, and overall mass transfer coefficient [24,27,28].

Furthermore, gas holdup is affected by the gas velocity, which is known as gas flow rate. As the gas flow rate increases, the gas holdup in the riser and downcomer increases, and as a result, the liquid circulation and bubble velocities increase. Larger bubbles move faster and descend to the downcomer, which results in better light absorption by cyanobacteria [29,30]. However, as the liquid velocity increases at higher gas flow rates, cyanobacteria do not remain in the downcomer long enough to utilize light efficiently [31] and may suffer from shear stress. Liquid velocity affects many hydrodynamic and mass transfer parameters, including average bubble residence time, bubble size, overall mass transfer rate, and mixing time. In addition, it influences turbulence, mass transfer coefficient, and shear stress [25,29]. As a result, there is a lack of data and studies on the effect of hydrodynamic parameters of the ALR (gas holdup, bubble diameter, and gas and liquid velocities) on the growth of cyanobacteria and CO_2 biofixation. Therefore, the present study aims at evaluating the CO_2 biofixation by *Spirulina* sp. through the optimization of gas flowrate, gas holdup, and liquid velocities in an airlift photobioreactor.

2. Materials and Methods

2.1. Algal Strain and Cultivation Conditions

Spirulina sp. strain was sourced from Science and Technology Park, Bushehr, Iran, and it was cultivated in BG-11 culture medium [32], which is described in Table 1. The stock

culture was maintained in a 500 mL Erlenmeyer flask containing 250 mL of the medium at 27 °C under 60 μmol m^{-2} s^{-1} of light intensity and a 12/12 h day/night cycle [15].

Table 1. Composition of BG-11 culture medium.

Stock Solution	Composition	Stock Solution g L^{-1}
Nutrient Solution of BG-11 culture medium	NaNO$_3$	1.5 g
	K$_2$HPO$_4$	0.04 g
	MgSO$_4$·7H$_2$O	0.075g
	CaCl$_2$·2H$_2$O	0.036 g
	citric acid	6.0 mg
	ferric ammonium citrate	6.0 mg
	Na$_2$EDTA	1.0 mg
	Na$_2$CO$_3$	0.02 g
Trace metals mix A5 (1 mL for 1 L BG-11)	H$_3$BO$_3$	2.86 g
	MnCl$_2$·4H$_2$O	1.81 g
	ZnSO$_4$·7H$_2$O	0.222 g
	Na$_2$MoO$_4$·2H$_2$O	0.39 g
	CuSO$_4$·5H$_2$O	0.079 g
	Co(NO$_3$)$_2$·6H$_2$O	49.4 mg

2.2. Airlift Photobioreactor Configuration

The airlift photobioreactor used in this experiment, as shown in Figure 1, was made of two vertical Plexiglas loops with a stainless-steel circular distributor installed at the bottom of the reactor. The distributor consisted of eighteen 1-mm holes placed at regular intervals.
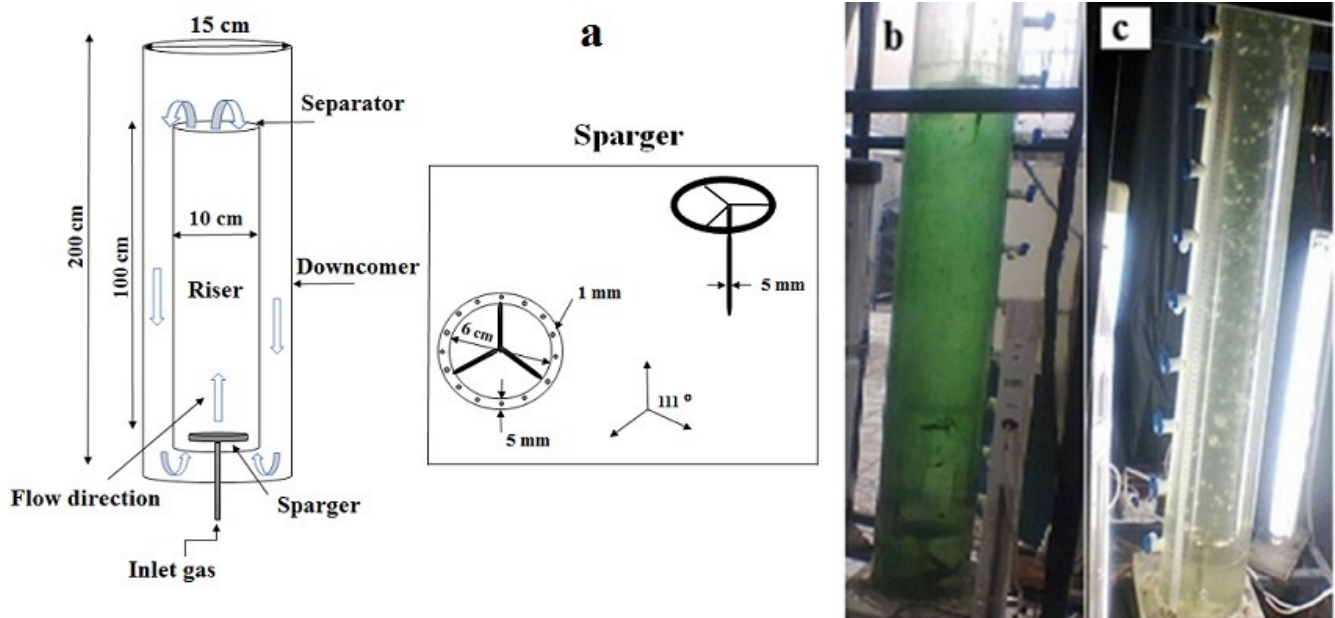

Figure 1. (**a**) Schematic diagram of the experimental setup; Images of (**b**) microalgae growth and (**c**) distilled water in the airlift photobioreactor.

The total volume and working volume of the reactor were 20 L and 16 L, respectively. To control the temperature at 30 °C, a 100-watt heater (Sobo HC-100 model) was fitted inside the reactor. Also, two gas rotameters were used to measure the air and carbon

dioxide flow rates. Illumination was provided using four fluorescent lamps, and light intensity was measured with a lux meter (TES-1339R, TES Taiwan, Taipei, Taiwan).

2.3. Hydrodynamic Tests in Distilled Water

Initially, the hydrodynamic parameters of ALR were investigated by performing gas holdup tests in distilled water only by varying the inlet gas velocity and measuring the average bubble size. For this purpose, experiments, which were repeated three times, conducted at six different gas velocities of (0.185, 0.524, 0.857, 1.176, 1.593, and 1.936 cm/s) (Table 2), to find out the range of the bubbly flow (homogenous regime) for optimum cyanobacterial growth.

Table 2. Hydrodynamic parameters tested in the ALR at different gas velocities.

Gas velocity (cm/s)	0.185	0.524	0.857	1.176	1.593	1.936
Gas holdup (cm/cm)						
Mean bubble diameter (mm)						
Bubble velocity (cm/s)						
Liquid circulation velocity in riser (cm/s)						
Liquid circulation velocity in downcomer (cm/s)						

2.4. Inoculation and Operation of the Photobioreactor

Spirulina sp. growth and CO_2 removal efficiency were studied after transferring 1.6 L of an acclimated culture of *Spirulina* sp. into the ALR and filling it with 14.4 L of culture medium. A mixture of 95% air and 5% (*v/v*) CO_2 [15,33] was sparged at the bottom of the reactor. Two separate experiments were carried out for 7 days at gas velocities of 0.185 and 0.524 cm/s corresponding to flow rates of 0.87 and 2.47 L/min or 0.054 and 0.154 volume of air per medium volume per minute (vvm), respectively. The initial concentration of cyanobacteria was about 0.5 g L^{-1}. The light intensity was 150 μmol photons m^{-2} s^{-1} with a 12:12 light-dark (LD) cycle, and the temperature was 30 ± 1 °C [15,34]. The pH of the culture medium was adjusted to 9.5 ± 0.02 using 6 M NaOH [19,35]. The pH was measured using a pH meter (Metrohm 827 pH Lab meter). BG-11 medium was added weekly from the top of the reactor equipped with a small tank with a one-way valve to compensate for water evaporation from the photobioreactor.

2.5. Gas Holdup and Bubble Size Measurements

The gas holdup is described as a fraction of a gas-filled reactor volume and calculated from the following Equation (1) [25]:

$$\varepsilon = \frac{H_2 - H_1}{H_2} \tag{1}$$

H_2 and H_1 are liquid heights after aeration and initial in the reactor, respectively.

This parameter affects the residence time of the gas phase in the liquid phase, and it influences the gas-liquid interface through bubble size. In this study, the total gas holdup test was performed using distilled water and air first, then with the cyanobacterial culture aerated with air and carbon dioxide. Since bubbles with different sizes exist in the dispersed phase, the Sauter mean bubble diameter (d_{32}), which is a sphere diameter with the same volume to surface ratio as the whole bubble size, was used in calculations and is determined by Equation (2) [25,36,37]:

$$d_{32} = \frac{\sum_{i=1}^{N} N_i d_i^3}{\sum_{i=1}^{N} N_i d_i^2} \tag{2}$$

In which N_i is the occurrence of the bubble with diameter d_i. Also, the bubble velocity was calculated using Equation (3) [25]:

$$U_b = \frac{U_g}{\varepsilon} \tag{3}$$

where U_g is the gas velocity.

In this experiment, the average bubble size was analyzed using Image J software.

2.6. Gas Velocity

The gas velocity directly impacts the gas holdup, which is more apparent in bubbly regimes than in turbulent flow. In the airlift reactor, the gas velocity is equal to the ratio of the gas inlet volume to the riser cross-section as shown in Equation (4) [36]:

$$U_g = \frac{G_g}{A_r} \tag{4}$$

where G_g and A_r are the inlet flow rate to the airlift reactor and riser cross-section, respectively.

2.7. Liquid Circulation Velocity

Due to the difference in fluid density between riser and downcomer in reactors, the fluid reaches a certain velocity [38]. The mean circulation velocity is defined by Equation (5) [39]:

$$U_{circ} = \frac{X_{circ}}{t_{circ}} \tag{5}$$

where x_c and t_c are the length of the circulation path and the mean circulation time, respectively, however, liquid velocity values in riser (U_r) and downcomer (U_d) are more useful than mean circulation velocity (U_{circ}). However, the liquid velocity in the riser is calculated with Equation (5) and the following correlation (Equation (6)) was used to determine the liquid velocity in the downcomer in which A_d and A_r are downcomer and riser cross-sections, respectively [39].

$$U_d \times A_d = U_r \times A_r \tag{6}$$

2.8. Calculation of CO_2 Removal Efficiency

To estimate the CO_2 removal efficiency, Equation (7) was used;

$$CO_2 \text{ removal efficiency } (\%) = \left(1 - \frac{CO_2 \text{ output}}{CO_2 \text{ input}}\right) \times 100 \tag{7}$$

where CO_2 input is the carbon dioxide concentration in the gas injected into the bioreactor, while CO_2 output is the concentration in ppm of carbon dioxide exiting the reactor. To measure CO_2 concentration in the headspace of the reactor, a CO_2 meter (Testo, Lenzkirch, Germany, model 535) was used.

2.9. Biomass Concentration

Each day, a 20 mL sample from the ALR was withdrawn to measure the growth medium optical density at 680 nm (OD_{680}) [15,40] using a spectrophotometer (DR 5000, Hach, Loveland, HQ, USA).

To obtain the dry cell weight, the sample was centrifuged at 2000 rpm for 15 min [41] using a centrifuge (Sigma 3-30KS, Sigma, Burlington, MA, USA). The residue was then placed in an oven for 72 h to remove moisture completely. Finally, the total dry weight of *Spirulina* sp. was measured.

Specific growth rate (μ, day^{-1}) was calculated according to Equation (8):

$$\mu = \frac{\ln(X_2) - \ln(X_1)}{\Delta t}$$ (8)

where X_2 and X_1 represent biomass concentration (g L^{-1}) during culture days t_1 and t_2. To estimate the biomass productivity (p, g L^{-1} day^{-1}), Equation (9) was used.

$$p = \frac{X_2 - X_1}{t_2 - t_1}$$ (9)

3. Results and Discussion

3.1. Gas Holdup and Bubble Behavior in Distilled Water

As shown in Figure 2, it was observed that an increase in the gas velocity from 0.185 to 1.936 cm/s resulted in a relatively small increase in gas holdup compared to other empirical correlations. To predict gas holdup in the ALR in the rage of gas velocity studied, theoretical correlations [42–46] which are presented in Table 3, were used. As in this study Equation (1) was used, factors such as gas and liquid densities (ρ_g and ρ_l), the surface tension of the liquid (σ) gas and liquid viscosities (μ_g and μ_l) and gravitational constant (g) were ignored, and as a result, there is a difference between measured gas holdup and predicted holdup using empirical correlations [42–45]. However, the experimental data obtained in this study is consistent with Hikita et al.'s correlation [46]. They confirmed that total gas holdup increases linearly with the inlet gas velocity in the range of velocity investigated. The reason for this was the change in the shape and nature of gas bubbles at a higher velocity of the inlet gas [30,47,48]. As gas velocity increased, bubble size also increased (larger bubbles were released from the sparger at the bottom), but as these large bubbles rose in the liquid column, they quickly broke down into small bubbles; as a result, the number of smaller bubbles increased and the mean bubble diameter decreased, which is presented in Table 4; also the accumulation of large bubbles in the center and small ones along the walls of the reactor was observed. Chisti reported that in the total gas holdup, the percentage of small bubbles is greater than large bubbles [49].
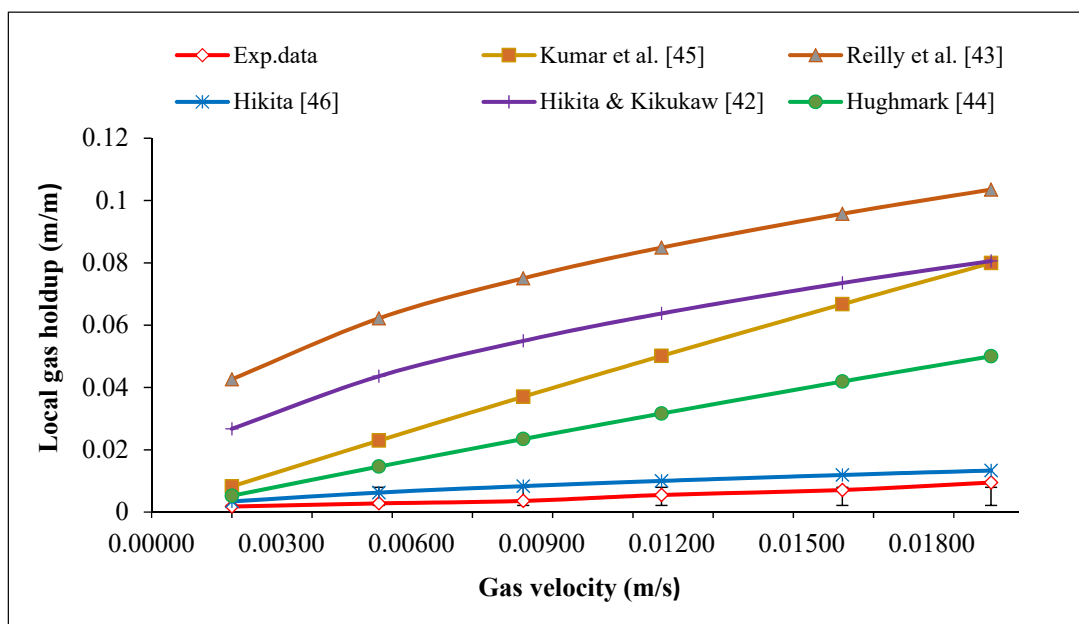

Figure 2. Comparison of gas holdup experimental data with empirical correlations [42–46].

Table 3. Theoretical correlations used in this study.

Hikita and Kikukaw [42]	$\varepsilon = 0.505u_g^{0.47}\left(\frac{0.072}{\sigma}\right)^{0.67}\left(\frac{0.001}{\mu_l}\right)^{0.05}$
Reilly et al. [43]	$\varepsilon = 0.009 + 296u_g^{0.44}\rho_l^{-0.98}\sigma_l^{-0.16}\rho_g^{0.19}$
Hughmark [44]	$\varepsilon = \frac{1}{2+(0.35/u_g)(\rho_l\sigma/72)^{0.33}}$
Kumar et al. [45]	$\varepsilon = 0.728u - 0.485u^2 + 0.0975u^3$ $u = u_g\left[\frac{\rho_l^2}{\sigma}(\rho_l - \rho_g)g\right]^{1/4}$
Hikita [46]	$\varepsilon = 0.672\left(u_g\mu_l\right)^{0.578}\left(\frac{\mu_l^4 g}{\sigma^3\rho_l}\right)^{-0.131}\left(\frac{\rho_g}{\rho_l}\right)^{0.062}\left(\frac{\mu_g}{\mu_l}\right)^{0.107}$

Table 4. Mean bubble diameter at different gas velocities in the airlift photobioreactor.

Gas velocity (cm/s)	0.185	0.524	0.857	1.176	1.593	1.936
Flow rate (L/min)	0.87	2.47	4.03	5.54	7.50	9.12
vvm	0.054	0.154	0.25	0.343	0.468	0.568
Mean bubble diameter in distilled water (mm)	12.8 ± 0.64	10.4 ± 0.52	9.9 ± 0.49	9.2 ± 0.46	5.9 ± 0.29	4.6 ± 0.23
Mean bubble diameter in microalgal culture (mm)	11.1	8.6	7.8	7.3	4.2	3.8

In Figure 3, the results of total gas holdup in cyanobacterial solution were compared with that obtained using distilled water (Figure 2). The mean bubble velocities in distilled water and cyanobacterial medium on the first and sixth days of cultivation were 109.97, 87.98, and 65.89 cm/s, respectively. Results indicated that the bubble velocity in both distilled water and cyanobacterial culture increased with increasing gas velocity, and bubbles were widely distributed. However, as the size of the bubbles directly influences the bubble velocity, higher bubble velocity was observed in distilled water compared to cyanobacterial culture due to a lower viscosity. This observation is in agreement with previous studies [50,51].
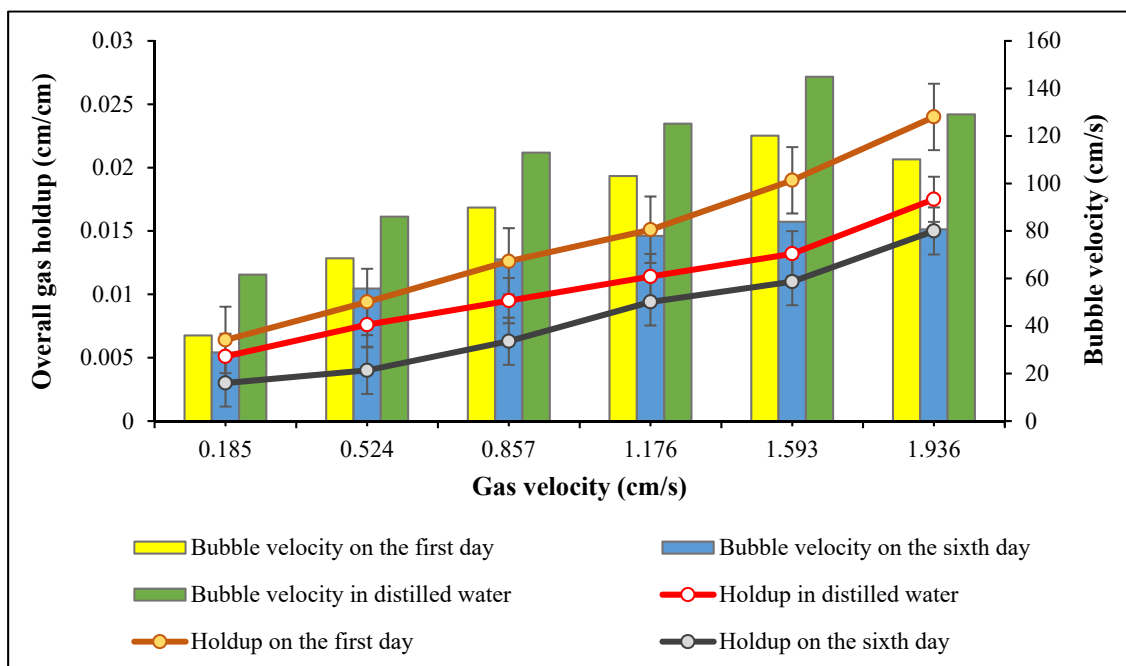
Figure 3. Comparison of gas holdup and bubble velocity at different gas velocities in distilled water, and on the first and sixth days of cyanobacterial growth in the reactor.

3.2. Gas Holdup in Cyanobacterial Culture

In the experiment using cyanobacterial culture, the total gas holdup was measured on two different days. The experimental results aligned with Equation (3), which clearly shows that the total holdup decreases when the bubble velocity increases at a constant gas velocity [25]. Also, the gas holdup on the first day was higher than in distilled water. According to Chisti [25], at the beginning of the cell growth, smaller bubbles are formed, which increase gas holdup. Also, the ions dissolved in the cyanobacterial culture medium prevented the bubbles from coalescing and forming larger bubbles [25]. As growth took place in the airlift reactor, the holdup decreased. On the sixth day, when *Spirulina* sp. was at its highest density, there was less turbulence in the ALR, resulting in a lower gas holdup, which is consistent with other works [22,36]. According to some researchers [52], gas holdup on the first day of microalgal growth was 48.7% higher than the holdup in distilled water, and with the increase in the liquid viscosity, holdup declined. Another study [53] investigated the impact of high liquid viscosity on gas holdup in a cylindrical split airlift photobioreactor. They observed a decline in the holdup with an increase in viscosity.

3.3. Liquid Circulation Velocity

The movement of gas bubbles pushes the liquid upwards in the riser and falls in the downcomer. As shown in Figure 4, the increase in the gas velocity resulted in an increase in the liquid velocity of the riser and downcomer, but these changes were faster at low gas velocities. This observation is in close agreement with other studies [39,54].
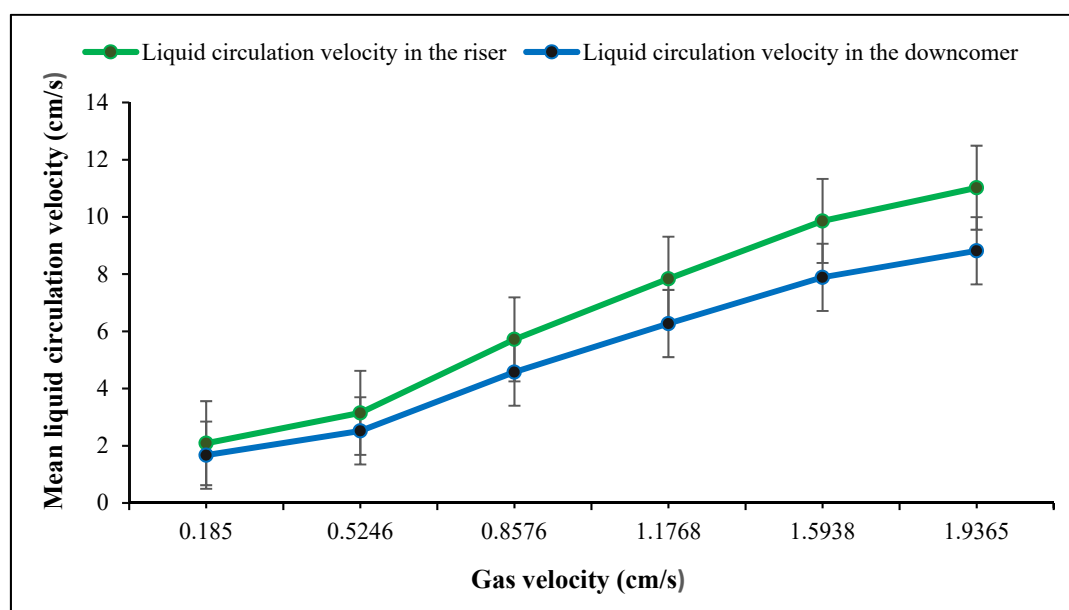

Figure 4. Comparison of liquid circulation velocity in the riser and downcomer at 6 different gas velocities.

3.4. Cyanobacterial Growth

It was observed that increasing the inlet gas velocity to 1.936 cm/s was detrimental as it resulted in a major decrease in cyanobacterial growth. The decline began at a flowrate of 0.857 cm/s when the flow became more turbulent. With the increase in the aeration rate, the mean bubble diameter gradually decreased from 11.1 to 3.8 mm (Table 4). As higher velocities caused more turbulence, the average bubble diameter was smaller due to micro-eddies, which caused small bubbles, and damaged cells which is in agreement with previous work [30]. It was reported that the mean bubble size is important for better cyanobacterial growth because with an increase in the bubble size, algal growth can also decline [25]. Moreover, Sadeghizadeh et al. studied the effect of input gas velocity on *Chlorella vulgaris* growth in an ALR, they found that with an increase in the gas velocity

over 0.74 cm/s biomass concentration declined [55]. As shown in Figures 5–7, the dry cell weight, specific growth rate and biomass productivity of *Spirulina* sp. were analyzed daily during separate experiments carried out at two different gas velocities (0.185, 0.524 cm/s). As shown in Figure 5, due to some settling in the reactor after the inoculation, the dry cell weight decreased on day 1 compared to day 0, also some cells got stuck on the reactor walls. However, the biomass concentration increased steadily during the culture period and reached a maximum dry cell weight of 1.62 g/L at the gas velocity of 0.524 cm/s, which is presented in Table 5. Increasing the aeration rate resulted in an increase in the gas holdup and fluid circulation rate, which improved the mass transfer and cyanobacterial growth in the bioreactor, which is in line with a previous study [39]. At 0.524 cm/s, the sedimentation rate reduced, and more cyanobacteria were suspended in the culture medium. As a result, cells had better exposure to light, which caused better light absorption, photosynthesis, and growth rate. Thus, 0.524 cm/s was considered a more suitable gas velocity for *Spirulina* sp. without damaging cells. It was also observed that there was a statistically significant difference between group means as determined by one-way ANOVA (F = 5.28414, p = 0.04029). In a similar study [30], which was carried out in a 50 L airlift photobioreactor using 5% input CO_2 and at a flow rate of 12.0 L/min, the maximum dry cell of *Chlorella protothecoides* was reported to be 0.24 g/L after 300 h. They found that when the aeration rate was 8.0 L/min, the final biomass concentration reached 0.32 g/L after 500 h (Table 5) highlighting the effect of the aeration rate on cell shear stress. Another work investigated the impact of increasing aeration rate from 0.145 vvm to 0.29 vvm with a mixture of 0.038% CO_2 and air on the growth rate of *C. vulgaris* in an ALR with a working volume of 80 L. The maximum biomass concentration of 1.42 g/L was achieved at an aeration rate of 0.29 vvm after 14 days (Table 5) [56]. Also, it was reported that the maximum biomass concentration of *Chlorella* sp. with a constant CO_2 concentration of 1.75% reached 2.8 g/L in a bubble column reactor after 13 days. They found that with an increase in the flow rate from 50 to 70 mL/min, the maximum biomass concentration of *Chlorella* sp. increased from 2.5 to 2.8 g/L (Table 5) [57].
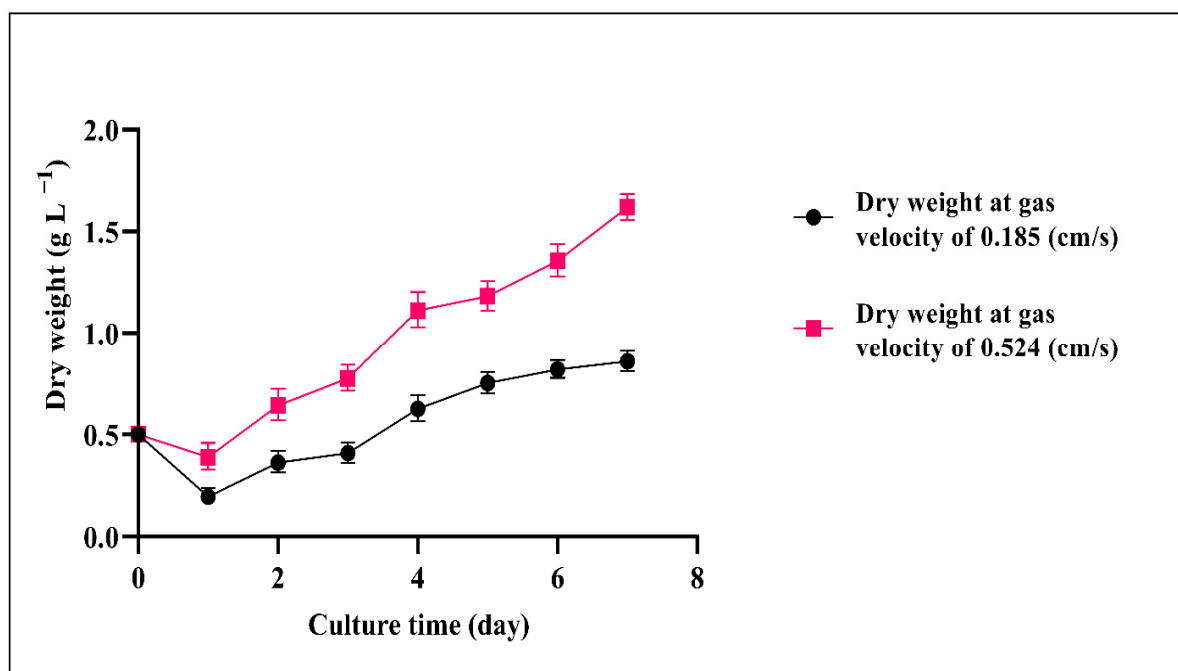

Figure 5. Dry weight of *Spirulina* sp. at two gas velocities (0.185, 0.524 cm/s), temperature 30 ± 1 °C and pH = 9.5 ± 0.02.
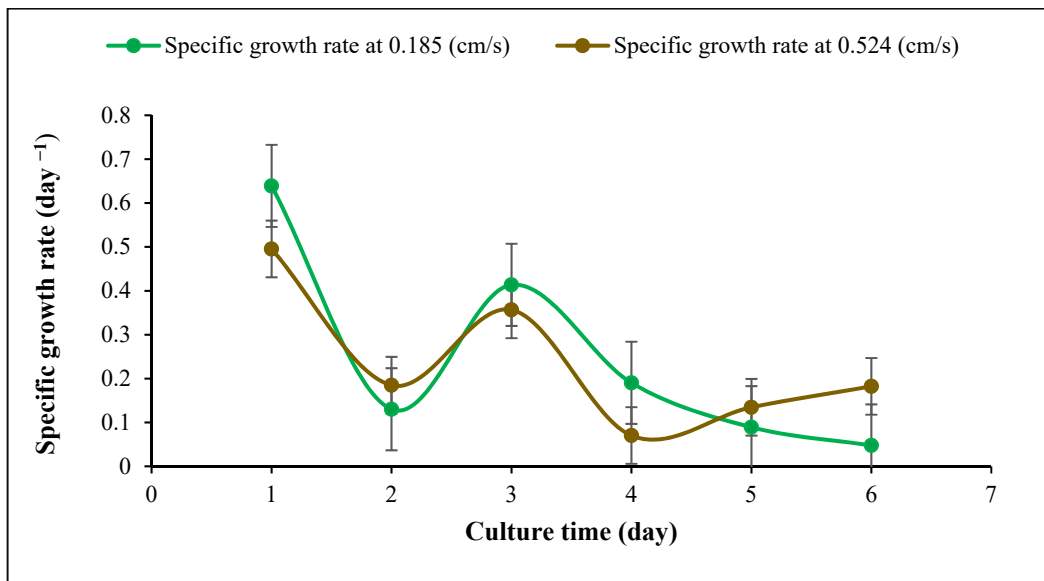
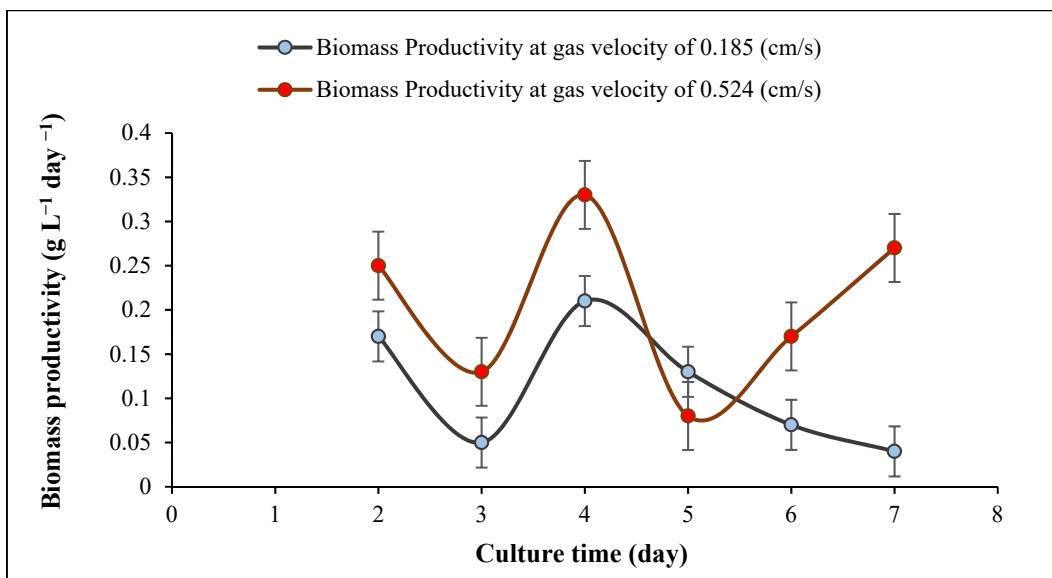**Figure 6.** Specific growth rate of *Spirulina* sp. at two gas velocities (0.185, 0.524 cm/s), temperature $30 \pm 1\,^{\circ}C$ and pH = 9.5 ± 0.02.

Figure 7. Biomass productivity of *Spirulina* sp. at two gas velocities (0.185, 0.524 cm/s), temperature $30 \pm 1\,^{\circ}C$ and pH = 9.5 ± 0.02.

3.5. CO_2 Removal

Figure 8 shows the carbon dioxide removal efficiency at each gas velocity during 7 days. The results demonstrated that during the first four days, the CO_2 removal efficiency for both velocities increased gradually; however, during the last three days, there was a sharp rise at the gas velocity of 0.185 cm/s. Although the gas velocity of 0.524 cm/s provided better gas-liquid mixing, recirculation, and cyanobacterial growth, the highest carbon dioxide removal efficiency (55.5%) (Table 5) was achieved at the gas velocity of 0.185 cm/s and a dry cell weight of 0.86 g/L. The results illustrated that there was a statistically significant difference between group means as determined by one-way ANOVA (F = 6.15675, p = 0.02889). This result indicated that higher CO_2 removal efficiency was achieved at the lower aeration rate for several reasons. Firstly, CO_2 capture efficiency can decrease because bubbles interconnect at higher gas velocity. Bubble surface area per unit volume of gas decreased,

and larger bubbles rose faster than smaller ones [22,58]; as a result, the CO_2 uptake from gas bubbles reduced, which is in agreement with previous research [49]. Secondly, when the inlet gas velocity increased, CO_2 fixation in the high-density culture (at higher viscosity) declined due to a decrease in gas retention time and CO_2 consumption [59]. In a study carried out at four flow rates (0.145, 0.195, 0.24, and 0.29 vvm) using *C. vulgaris* in an airlift reactor, it was found that CO_2 removal efficiency decreased from 28% at 0.145 vvm to 2% at 0.29 vvm (Table 5) due to a shorter residence time at higher gas velocity [56]. Also, it was reported that at two inlet gas velocities (0.74 and 1.32 cm/s) with 2% CO_2 in an ALR, the maximum CO_2 removal efficiency of *C. vulgaris* was 80% at 0.74 cm/s (Table 5) [55]. A similar work carried out in a bubble column reactor by sparging 4% CO_2 indicated that with the increase in superficial gas velocity from 0.10 to 0.50 cm/s, the CO_2 removal efficiency of *C. vulgaris* declined from 14.6% to 3.8% (Table 5) [60]. Li et al. [61] also studied the impact of increasing gas aeration rate on CO_2 removal efficiency of *Scenedesmus obliquus* WUST4 enriched with 12% CO_2 in an airlift photobioreactor and found that the maximum CO_2 removal efficiency was 67%, which was achieved at a flow rate of 0.1 vvm, but it decreased to 20% when increasing the aeration rate to 0.5 vvm (Table 5). However, some authors [58] claimed that increasing cell density, which led to an increase in the culture viscosity, decreased CO_2 concentration in the headspace of the reactor due to an increase in the gas retention time and carbon dioxide consumption. Nevertheless, with the increase in biomass concentration, the amount of light absorbed by cells diminished due to the higher viscosity of the culture medium. It means that the available light limits the rate of photosynthesis, which in turn reduces the CO_2 consumed by microalgae [62]. Our results are consistent with the previous work carried out by Pourjamshidian et al. [57], where the authors observed that the highest CO_2 removal efficiency of *Chlorella* sp. was 95.45% at a flow rate of 50 mL/min, and this declined to 88.63% at an aeration rate of 70 mL/min due to a limited algal photosynthetic capacity (Table 5).
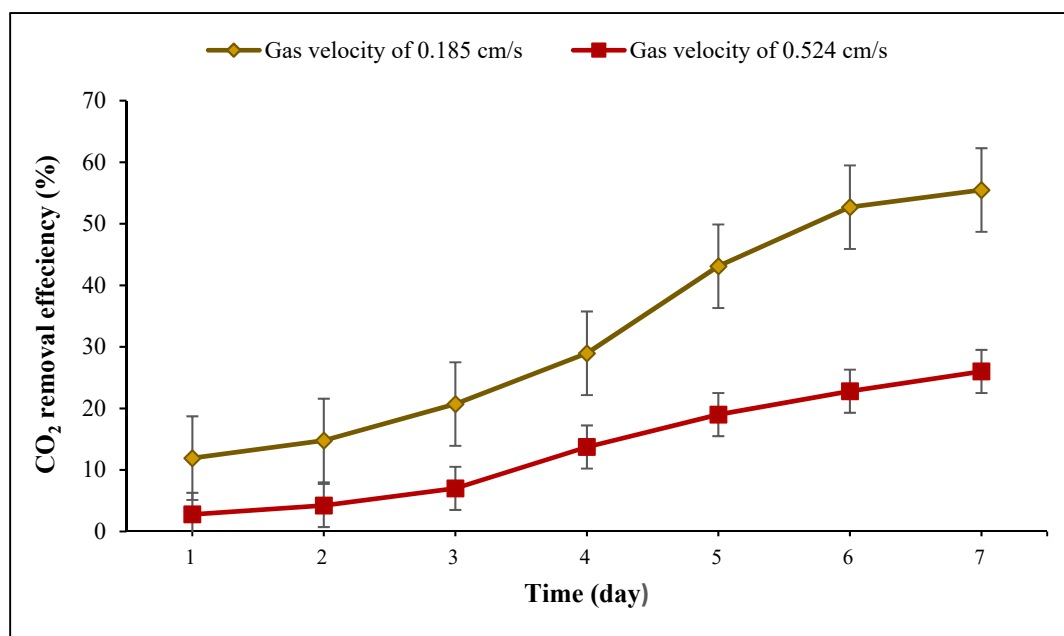

Figure 8. CO_2 removal efficiencies at gas velocities of (0.185 and 0.524 cm/s) during the growth of *Spirulina* sp. (temperature 30 $\pm$ 1 °C; pH = 9.5 $\pm$ 0.02).

Table 5. Summary of present study's results with other works.

Gas Velocity	CO$_2$ Concentration (%)	Species	Maximum CO$_2$ Removal Efficiency (%)	Maximum Dry Weight (g L^{-1})	Maximum Specific Growth Rate (day^{-1})	Maximum Biomass Productivity (g L^{-1} day^{-1})	Reference
0.185 cm/s [1] 0.524 cm/s	5%	*Spirulina* sp.	55.5% 23%	0.86 1.62 (after 7 days)	0.63 0.50	0.21 0.33	This study
8.0 L/min 12.0 L/min	5%	*Chlorella protothecoides*	- -	0.32 (after 500 h) 0.24 (after 300 h)	- -	- -	[30]
0.145 vvm 0.29 vvm	0.038%	*Chlorella vulgaris*	28% 2%	- 1.42 (after 14 days)	- 0.16	- -	[56]
50 mL/min 70 mL/min	1.75%	*Chlorella* sp.	95.45% 88.63%	2.5 (after 12 days) 2.8 (after 13 days)	1.11 1.00	- 0.17	[57]
0.74 cm/s 1.32 cm/s	2%	*C. vulgaris*	80% 64%	- -	0.24 0.18 (after 11 days)	- -	[55]
0.10 cm/s 0.50 cm/s	4%	*C. vulgaris*	14.6% 3.8%	2.7 3.6 (after 10 days)	- -	0.41 0.47	[60]
0.1 vvm 0.5 vvm	12%	*Scenedesmus obliquus* WUST4	67% 21%	- -	- -	- -	[61]

[1] To compare the gas velocity with the flow rate or vvm, the data was collected in Table 4.

3.6. Perspective

Due to the increase in CO$_2$ emissions and demand for better climate policies, this airlift reactor can be used in large scale. This is a cost-effective, sustainable way to capture carbon dioxide. Moreover, the results of this research illustrated that this airlift reactor was suitable for production of *Spirulina* biomass which is used in wide range.

4. Conclusions

This study demonstrated that the presence of cyanobacteria influenced the bubble velocity and gas holdup compared to the air-water system. It was observed that with an increase in the inlet gas velocity in the cyanobacterial culture, holdup and bubble velocity increased but more slowly than in the air-water system. Also, the inlet gas velocity and the average bubble size had a major impact on cyanobacterial growth and CO$_2$ uptake. At higher gas velocity, there was a decrease in cyanobacterial growth due to the interaction between bubbles and cells; as a result, the optimal gas velocity for *Spirulina* sp. growth was achieved at 0.524 cm/s. However, the maximum carbon dioxide efficiency (55.5%) was observed at the lower gas velocity (0.185 cm/s) due to the higher surface area of bubbles and longer residence time in the lower viscosity of the culture. Although CO$_2$ removal efficiency needs more investigation regarding different hydrodynamic parameters in the airlift photobioreactor, this study showed the feasibility of the CO$_2$ biofixation process using *Spirulina* sp.

References

1. Wang, X.; Jiang, D.; Lang, X. Future extreme climate changes linked to global warming intensity. *Sci. Bull.* **2017**, *62*, 1673–1680. [CrossRef]
2. Hansen, J.; Sato, M.; Ruedy, R.; Lo, K.; Lea, D.W.; Medina-Elizade, M. Global temperature change. *Proc. Natl. Acad. Sci. USA* **2006**, *103*, 14288–14293. [CrossRef] [PubMed]
3. Blasing, T.; Smith, K. Recent Greenhouse Gas Concentrations. Available online: https://cdiac.ess-dive.lbl.gov/pns/current_ghg (accessed on 13 April 2016). [CrossRef]
4. Prazeres, A.R.; Rivas, J.; Paulo, Ú.; Ruas, F.; Carvalho, F. Sustainable treatment of different high-strength cheese whey wastewaters: An innovative approach for atmospheric CO_2 mitigation and fertilizer production. *Environ. Sci. Pollut. Res.* **2016**, *23*, 13062–13075. [CrossRef] [PubMed]
5. Yadav, G.; Sen, R. Microalgal green refinery concept for biosequestration of carbon-dioxide vis-à-vis wastewater remediation and bioenergy production: Recent technological advances in climate research. *J. CO₂ Util.* **2017**, *17*, 188–206. [CrossRef]
6. Chaudhary, R.; Dikshit, A.K.; Tong, Y.W. Carbon-dioxide biofixation and phycoremediation of municipal wastewater using *Chlorella vulgaris* and *Scenedesmus obliquus*. *Environ. Sci. Pollut. Res.* **2018**, *25*, 20399–20406. [CrossRef]
7. Pires, J.C.M.; Alvim-Ferraz, M.C.M.; Martins, F.G.; Simões, M. Carbon dioxide capture from flue gases using microalgae: Engineering aspects and biorefinery concept. *Renew. Sustain. Energy Rev.* **2012**, *16*, 3043–3053. [CrossRef]
8. Karemore, A.; Ramalingam, D.; Yadav, G.; Subramanian, G.; Sen, R. *Photobioreactors for Improved Algal Biomass Production: Analysis and Design Considerations*; Springer: Cham, Switzerland, 2015; pp. 103–124.
9. Almomani, F.; Al Ketife, A.; Judd, S.; Shurair, M.; Bhosale, R.R.; Znad, H.; Tawalbeh, M. Impact of CO_2 concentration and ambient conditions on microalgal growth and nutrient removal from wastewater by a photobioreactor. *Sci. Total Environ.* **2019**, *662*, 662–671. [CrossRef]
10. Zhao, B.; Su, Y. Process effect of microalgal-carbon dioxide fixation and biomass production: A review. *Renew. Sustain. Energy Rev.* **2014**, *31*, 121–132. [CrossRef]
11. Sevda, S.; Bhattacharya, S.; Reesh, I.M.A.; Bhuvanesh, S.; Sreekrishnan, T.R. Challenges in the Design and Operation of an Efficient Photobioreactor for Microalgae Cultivation and Hydrogen Production. In *Biohydrogen Production: Sustainability of Current Technology and Future Perspective*; Singh, A., Rathore, D., Eds.; Springer: New Delhi, India, 2017; pp. 147–162.
12. Bhola, V.; Swalaha, F.; Ranjith Kumar, R.; Singh, M.; Bux, F. Overview of the potential of microalgae for CO_2 sequestration. *Int. J. Environ. Sci. Technol.* **2014**, *11*, 2103–2118. [CrossRef]
13. Jung, J.-Y.; Yang, J.-W.; Kim, K.; Hwang, K.-T.; Jung, S.M.; Kwon, J.-H. Cost-efficient cultivation of *Spirulina platensis* by chemical absorption of CO_2 into medium containing NaOH. *Korean J. Chem. Eng.* **2015**, *32*, 2285–2289. [CrossRef]
14. Morais, E.G.d.; Cassuriaga, A.P.A.; Callejas, N.; Martinez, N.; Vieitez, I.; Jachmanián, I.; Santos, L.O.; Morais, M.G.D.; Costa, J.A.V. Evaluation of CO_2 biofixation and biodiesel production by *Spirulina* (*Arthospira*) cultivated in air-lift photobioreactor. *Braz. Arch. Biol. Technol.* **2018**, *61*. [CrossRef]
15. Ramirez-Perez, J.C.; Janes, H. Impact of salinity on the kinetics of CO_2 fixation by *Spirulina platensis* cultivated in semi-continuous photobioreactors. *Eclética Química J.* **2021**, *46*, 21–34. [CrossRef]
16. de Morais, M.G.; Costa, J.A.V. Biofixation of carbon dioxide by *Spirulina* sp. and *Scenedesmus obliquus* cultivated in a three-stage serial tubular photobioreactor. *J. Biotechnol.* **2007**, *129*, 439–445. [CrossRef] [PubMed]
17. Watanabe, Y.; de la Noüe, J.; Hall, D.O. Photosynthetic performance of a helical tubular photobioreactor incorporating the cyanobacterium *Spirulina platensis*. *Biotechnol. Bioeng.* **1995**, *47*, 261–269. [CrossRef]
18. Singh, S.K.; Rahman, A.; Dixit, K.; Nath, A.; Sundaram, S. Evaluation of promising algal strains for sustainable exploitation coupled with CO_2 fixation. *Environ. Technol.* **2016**, *37*, 613–622. [CrossRef]
19. Soletto, D.; Binaghi, L.; Ferrari, L.; Lodi, A.; Carvalho, J.; Zilli, M.; Converti, A. Effects of carbon dioxide feeding rate and light intensity on the fed-batch pulse-feeding cultivation of *Spirulina platensis* in helical photobioreactor. *Biochem. Eng. J.* **2008**, *39*, 369–375. [CrossRef]
20. Vasumathi, K.K.; Premalatha, M.; Subramanian, P. Parameters influencing the design of photobioreactor for the growth of microalgae. *Renew. Sustain. Energy Rev.* **2012**, *16*, 5443–5450. [CrossRef]
21. Wang, B.; Lan, C.Q.; Horsman, M. Closed photobioreactors for production of microalgal biomasses. *Biotechnol. Adv.* **2012**, *30*, 904–912. [CrossRef]
22. Chisti, Y. *Pneumatically Agitated Bioreactors in Industrial and Environmental Bioprocessing: Hydrodynamics, Hydraulics, and Transport Phenomena*; ISME: Bangalore, India, 1998.
23. Pourtousi, M.; Ganesan, P.; Sandaran, S.C.; Sahu, J. Effect of ring sparger diameters on hydrodynamics in bubble column: A numerical investigation. *J. Taiwan Inst. Chem. Eng.* **2016**, *69*, 14–24. [CrossRef]
24. Wadaugsorn, K.; Limtrakul, S.; Vatanatham, T.; Ramachandran, P.A. Hydrodynamic behaviors and mixing characteristics in an internal loop airlift reactor based on CFD simulation. *Chem. Eng. Res. Des.* **2016**, *113*, 125–139. [CrossRef]
25. Chisti, M.Y. *Airlift Bioreactors*; Elsevier Applied Science: London, UK, 1989.
26. Ugwu, C.; Aoyagi, H.; Uchiyama, H. Photobioreactors for mass cultivation of algae. *Bioresour. Technol.* **2008**, *99*, 4021–4028. [CrossRef] [PubMed]
27. Guo, X.; Yao, L.; Huang, Q. Aeration and mass transfer optimization in a rectangular airlift loop photobioreactor for the production of microalgae. *Bioresour. Technol.* **2015**, *190*, 189–195. [CrossRef] [PubMed]

28. Mubarak, M.; Shaija, A.; Pranshanth, P. Bubble column photobioreactor for *Chlorella pyrenoidosa* cultivation and validating gas hold up and volumetric mass transfer coefficient. *Energy Sources Part A Recovery Util. Environ. Eff.* **2019**, 1–15. [CrossRef]

29. Rengel, A.; Zoughaib, A.; Dron, D.; Clodic, D. Hydrodynamic study of an internal airlift reactor for microalgae culture. *Appl. Microbiol. Biotechnol.* **2012**, *93*, 117–129. [CrossRef]

30. Ding, N.; Li, C.; Wang, T.; Guo, M.; Mohsin, A.; Zhang, S. Evaluation of an enclosed air-lift photobioreactor (ALPBR) for biomass and lipid biosynthesis of microalgal cells grown under fluid-induced shear stress. *Biotechnol. Biotechnol. Equip.* **2021**, *35*, 139–149. [CrossRef]

31. Sánchez Mirón, A.; García Camacho, F.; Contreras Gómez, A.; Grima, E.M.; Chisti, Y. Bubble-column and airlift photobioreactors for algal culture. *AIChE J.* **2000**, *46*, 1872–1887. [CrossRef]

32. Mohadi, R.; Mohadi, R.; Hermansyah, H.; Mavala, H.; Zulkifli, H. The effect of metal ion Cd(II) concentration on the growth of *Spirulina* sp. cultured on BG-11 medium. *IOP Conf. Ser. Earth Environ. Sci.* **2020**, *530*, 012036. [CrossRef]

33. Liu, H.; Chen, H.; Wang, S.; Liu, Q.; Li, S.; Song, X.; Huang, J.; Wang, X.; Jia, L. Optimizing light distribution and controlling biomass concentration by continuously pre-harvesting *Spirulina platensis* for improving the microalgae production. *Bioresour. Technol.* **2018**, *252*, 14–19. [CrossRef]

34. Mousavi, S.; Najafpour, G.D.; Mohammadi, M. CO_2 bio-fixation and biofuel production in an airlift photobioreactor by an isolated strain of microalgae *Coelastrum* sp. SM under high CO_2 concentrations. *Environ. Sci. Pollut. Res.* **2018**, *25*, 30139–30150. [CrossRef]

35. Sánchez-Luna, L.D.; Bezerra, R.P.; Matsudo, M.C.; Sato, S.; Converti, A.; de Carvalho, J.C. Influence of pH, temperature, and urea molar flowrate on *Arthrospira platensis* fed-batch cultivation: A kinetic and thermodynamic approach. *Biotechnol. Bioeng.* **2007**, *96*, 702–711. [CrossRef]

36. Zhang, W.; Yumei, Y.; Zhang, G.; Chao, Y.; Zaisha, M. Mixing characteristics and bubble behavior in an airlift internal loop reactor with low aspect ratio. *Chin. J. Chem. Eng.* **2014**, *22*, 611–621. [CrossRef]

37. Dejaloud, A.; Vahabzadeh, F.; Habibi, A. Hydrodynamics and oxygen transfer characterization in a net draft tube airlift reactor with water-in-diesel microemulsion. *Fuel Processing Technol.* **2018**, *171*, 265–276. [CrossRef]

38. Doran, P.M. Chapter 14—Reactor Engineering. In *Bioprocess Engineering Principles*, 2nd ed.; Doran, P.M., Ed.; Academic Press: London, UK, 2013; pp. 761–852.

39. Chisti, M.; Halard, B.; Moo-Young, M. Liquid circulation in airlift reactors. *Chem. Eng. Sci.* **1988**, *43*, 451–457. [CrossRef]

40. Cadondon, J.G.; Ong, P.M.B.; Vallar, E.A.; Shiina, T.; Galvez, M.C.D. Chlorophyll-a Pigment Measurement of *Spirulina* in Algal Growth Monitoring Using Portable Pulsed LED Fluorescence Lidar System. *Sensors* **2022**, *22*, 2940. [CrossRef]

41. Karthikeyan, D.; Muthukumaran, M.; Balakumar, B. Mass cultivation of microalgae in open raceway pond for biomass and biochemicals production. *Int. J. Adv. Res. Biol. Sci.* **2016**, *3*, 247–260.

42. Hikita, H.; Kikukawa, H. Liquid-phase mixing in bubble columns: Effect of liquid properties. *Chem. Eng. J.* **1974**, *8*, 191–197. [CrossRef]

43. Reilly, I.G.; Scott, D.S.; Bruijn, T.J.W.D.; Jain, A.K.; Piskorz, J. A correlation for gas holdup in turbulent coalescing bubble columns. *Can. J. Chem. Eng.* **1986**, *64*, 705–717. [CrossRef]

44. Hughmark, G. Holdup and mass transfer in bubble columns. *Ind. Eng. Chem. Process Des. Dev.* **1967**, *6*, 218–220. [CrossRef]

45. Kumar, A.; Degaleesan, T.E.; Laddha, G.S.; Hoelscher, H.E. Bubble swarm characteristics in bubble columns. *Can. J. Chem. Eng.* **1976**, *54*, 503–508. [CrossRef]

46. Hikita, H.; Asai, S.; Tanigawa, K.; Segawa, K.; Kitao, M. Gas hold-up in bubble columns. *Chem. Eng. J.* **1980**, *20*, 59–67. [CrossRef]

47. Choi, K.H.; Kim, J.W.; Lee, W.K. Bubble properties and mixing characteristics in an airlift bubble column with redistributor. *Korean J. Chem. Eng.* **1986**, *3*, 127–134. [CrossRef]

48. Tao, F.; Ning, S.; Zhang, B.; Jin, H.; He, G. Simulation Study on Gas Holdup of Large and Small Bubbles in a High Pressure Gas–Liquid Bubble Column. *Processes* **2019**, *7*, 594. [CrossRef]

49. Blažej, M.; Kiša, M.; Markoš, J. Scale influence on the hydrodynamics of an internal loop airlift reactor. *Chem. Eng. Proc. Proc. Intensif.* **2004**, *43*, 1519–1527. [CrossRef]

50. Deng, Z.; Wang, T.; Zhang, N.; Wang, Z. Gas holdup, bubble behavior and mass transfer in a 5m high internal-loop airlift reactor with non-Newtonian fluid. *Chem. Eng. J.* **2010**, *160*, 729–737. [CrossRef]

51. Ojha, A. *Advancing Microalgae Culturing via Bubble Dynamics, Mass Transfer, and Dynamic Growth Investigations*; Missouri University of Science and Technology: Park Hall, MI, USA, 2016.

52. Ojha, A.; Al-Dahhan, M. Local gas holdup and bubble dynamics investigation during microalgae culturing in a split airlift photobioreactor. *Chem. Eng. Sci.* **2018**, *175*, 185–198. [CrossRef]

53. Sabri, L.S.; Sultan, A.J.; Al-Dahhan, M.H. Investigating the cross-sectional gas holdup distribution in a split internal-loop photobioreactor during microalgae culturing using a sophisticated computed tomography (CT) technique. *Chem. Eng. Res. Des.* **2019**, *149*, 13–33. [CrossRef]

54. Kilonzo, P.M.; Margaritis, A.; Bergougnou, M. Hydrodynamics and mass transfer characteristics in an inverse internal loop airlift-driven fibrous-bed bioreactor. *Chem. Eng. J.* **2010**, *157*, 146–160. [CrossRef]

55. Sadeghizadeh, A.; Farhad dad, F.; Moghaddasi, L.; Rahimi, R. CO_2 capture from air by *Chlorella vulgaris* microalgae in an airlift photobioreactor. *Bioresour. Technol.* **2017**, *243*, 441–447. [CrossRef]

56. Alhaboubi, N. CO_2 sequestration using a novel Belt Conveyor Reactor with rotating sieve trays compared with Airlift Bubble Column as photobioreactors. *J. King Saud Univ. Eng. Sci.* **2021**, *in press*. [CrossRef]

57. Pourjamshidian, R.; Abolghasemi, H.; Esmaili, M.; Amrei, H.D.; Parsa, M.; Rezaei, S. Carbon dioxide biofixation by *Chlorella* sp. In a bubble column reactor at different flow rates and CO_2 concentrations. *Braz. J. Chem. Eng.* **2019**, *36*, 639–645. [CrossRef]

58. Chiu, S.-Y.; Kao, C.-Y.; Chen, C.-H.; Kuan, T.-C.; Ong, S.-C.; Lin, C.-S. Reduction of CO_2 by a high-density culture of *Chlorella* sp. in a semicontinuous photobioreactor. *Bioresour. Technol.* **2008**, *99*, 3389–3396. [CrossRef] [PubMed]

59. Pichler, T.; Stoppacher, B.; Kaufmann, A.; Siebenhofer, M.; Kienberger, M. Continuous Neutralization of NaOH Solution with CO_2 in an Internal-Loop Airlift Reactor. *Chem. Eng. Technol.* **2021**, *44*, 38–47. [CrossRef]

60. Hulatt, C.J.; Thomas, D.N. Productivity, carbon dioxide uptake and net energy return of microalgal bubble column photobioreactors. *Bioresour. Technol.* **2011**, *102*, 5775–5787. [CrossRef] [PubMed]

61. Li, F.-F.; Yang, Z.-H.; Zeng, R.; Yang, G.; Chang, X.; Yan, J.-B.; Hou, Y.-L. Microalgae Capture of CO_2 from Actual Flue Gas Discharged from a Combustion Chamber. *Ind. Eng. Chem. Res.* **2011**, *50*, 6496–6502. [CrossRef]

62. Contreras, A.; García, F.; Molina, E.; Merchuk, J. Interaction between CO_2-mass transfer, light availability, and hydrodynamic stress in the growth of *Phaeodactylum tricornutum* in a concentric tube airlift photobioreactor. *Biotechnol. Bioeng.* **1998**, *60*, 317–325. [CrossRef]